Characteristics of impact ionization rates in direct and indirect gap semiconductors

D. Harrison, R. A. Abram,[a] and S. Brand
Department of Physics, University of Durham, South Road, Durham DH1 3LE, United Kingdom

(Received 6 November 1998; accepted for publication 22 February 1999)

Impact ionization rates for electrons and holes in three semiconductors with particular band structure characteristics are examined to determine underlying factors influencing their qualitative behavior. The applicability of the constant matrix element approximation is investigated, and found to be good for the indirect gap material studied, but overestimates threshold softness in the direct gap materials. The effect that final states in the Γ valley have in influencing characteristics of the rate in the direct gap materials is investigated, and it is found that they play a significantly greater role than the low density of Γ valley states would suggest. The role of threshold anisotropy in affecting threshold softness is examined, and it is concluded that it plays only a small part, and that softness is controlled mainly by the slow increase in available phase space as the threshold energy is exceeded. © *1999 American Institute of Physics.* [S0021-8979(99)06411-7]

I. INTRODUCTION

Impact ionization is an important process occurring in devices in which significant numbers of high energy carriers are present. A carrier excited to high energy, typically by a high electric field, is able to excite a valence band electron across the band gap, thus creating an electron–hole pair. The process is often detrimental to device performance, limiting the bias at which devices such as field effect transistors can be operated,[1–3] whereas other devices such as IMPATT diodes[4] and avalanche photodiodes[5,6] rely on the charge multiplication it produces for their operation.

Monte Carlo simulation is a frequently used tool for theoretical investigations into the role of impact ionization in devices.[7–14] The rate of charge multiplication occurring in the simulation is affected by two factors: the process by which carriers are excited to high enough energies to initiate ionization, and the rate at which carriers that have gained sufficient energy actually ionize. In both these aspects of the calculation, the high energy nature of the process requires the use of realistic band structure. The resulting numerical complexity places large demands on computational resources and does not promote a simple understanding of the process. This paper is concerned with the second factor affecting impact ionization in devices—the rate of ionization initiated by carriers above threshold. In an effort to find more intuitive shortcuts to understanding the qualitative behavior of the impact ionization rate in different materials, rates in three semiconductors are examined in this paper with the aim of highlighting the underlying physical factors affecting their qualitative form.

II. METHOD

Impact ionization rates are calculated here in the semiclassical Fermi's Golden Rule approximation. The rate of transition for two electrons initially in states at $\mathbf{k}_1$ (the impacting electron) and $\mathbf{k}_2$ (the impacted electron) to final states at $\mathbf{k}_{1'}$ and $\mathbf{k}_{2'}$, given by Fermi's Golden Rule is[15]

$$R_{II}(\mathbf{k}_1,\mathbf{k}_2,\mathbf{k}_{1'},\mathbf{k}_{2'})=\frac{2\pi}{\hbar}|M_{if}|^2\delta(E_{1'}+E_{2'}-E_1-E_2), \tag{1}$$

where E_1, E_2, $E_{1'}$ and $E_{2'}$ are the energies of the electrons at $\mathbf{k}_1$, $\mathbf{k}_2$, $\mathbf{k}_{1'}$ and $\mathbf{k}_{2'}$ respectively. The matrix element is given by[15,16]

$$M_{if}=M_d-M_e, \tag{2}$$

where the so called direct matrix element M_d is given by

$$M_d=\int \psi_{1'}^*(\mathbf{r}_1)\psi_{2'}^*(\mathbf{r}_2)V\psi_1(\mathbf{r}_1)\psi_2(\mathbf{r}_2)d^3\mathbf{r}_1\,d^3\mathbf{r}_2, \tag{3}$$

$$V(\mathbf{r}_1,\mathbf{r}_2)=\frac{e^2}{(2\pi)^3\epsilon_0}\int\frac{e^{i\mathbf{q}\cdot(\mathbf{r}_2-\mathbf{r}_1)}}{\epsilon(\mathbf{q},\omega)|\mathbf{q}|^2}d^3\mathbf{q}, \tag{4}$$

$$\mathbf{q}=\mathbf{k}_{1'}-\mathbf{k}_1, \quad \hbar\omega=E_1-E_{1'}, \tag{5}$$

and the so called exchange matrix element M_e is obtained by exchanging the indices $1'$ and $2'$ in Eqs. (3) and (5).

Matrix elements are calculated using the pseudowave functions returned by the nonlocal pseudopotential method of Chelikowski and Cohen[17] which includes the effect of the spin-orbit interaction. The pseudowave functions are expanded in terms of 65 plane waves (130 expansion coefficients in all when spin is included). An isotropic q- and ω-dependent expression is used to approximate the full $\mathbf{q}$- and ω-dependent dielectric function $\epsilon(\mathbf{q},\omega)$ which appears in Eq. (4) and is calculated using the method of Walter and Cohen.[18]

To obtain the total transition rate from a given impacting state $\mathbf{k}_1$, all possible transitions must be summed over

$$R_{II}(\mathbf{k}_1)=\frac{\Omega^2}{(2\pi)^2}\int\frac{2\pi}{\hbar}|M_{if}|^2\delta(\Delta E)d^3\mathbf{k}_{1'}d^3\mathbf{k}_{2'}, \tag{6}$$

[a]Electronic mail: R.A.Abram@durham.ac.uk

TABLE I. Material parameters for the pseudopotential band structure calculation (see Ref. 17). V_S, V_A are symmetric and antisymmetric form factors in Ry; α_0, β_0 specify s-well depth in same way as in Ref. 17; R_0 is s-well radius in Å; A_2 is d-well depth in Ry; R_2 is d-well radius in Å; superscripts c and a denote cation and anion; α is ratio of spin splitting in free atoms; μ parametrizes strength of spin-orbit interaction in crystal and is adjusted to give spin split-off gaps of 0.35 eV in GaAs, 0.36 eV in InGaAs and 0.12 eV in SiGe.

Parameter	GaAs	InGaAs	SiGe
$V_S(\sqrt{3})$	−0.214	−0.2064	−0.2255
$V_S(\sqrt{8})$	0.014	0.0065	0.0268
$V_S(\sqrt{11})$	0.067	0.0558	0.0641
$V_A(\sqrt{3})$	0.055	0.0480	0.0000
$V_A(\sqrt{4})$	0.038	0.0441	0.0000
$V_A(\sqrt{11})$	0.001	0.0092	0.0000
α_0^c	0.000	0.0000	0.0036
β_0^c	0.000	0.0005	0.2008
A_2^c	0.125	0.5575	0.5262
R_0^c	1.296	1.2696	1.0596
R_2^c	1.219	1.2691	1.1982
α_0^a	0.000	0.0000	0.0036
β_0^a	0.000	0.1287	0.2008
A_2^a	0.625	1.5583	0.5262
R_0^a	1.058	1.0580	1.0596
R_2^a	1.219	1.2691	1.1982
α	1.380	0.9927	1.0000
μ	see caption	see caption	see caption
a_0	5.648	5.8618	5.5344

where

$$\Delta E = E(\mathbf{k}_{1'}) + E(\mathbf{k}_{2'}) - E(\mathbf{k}_1) - E(\mathbf{k}_{1'} + \mathbf{k}_{2'} - \mathbf{k}_1). \quad (7)$$

For each final state phase space element $d\mathbf{k}_{1'}\, d\mathbf{k}_{2'}$, the impacted vector $\mathbf{k}_2$ is chosen so as to ensure crystal momentum is conserved, and the Dirac delta function ensures energy is conserved in each transition. The six-dimensional integral is performed by an algorithm described elsewhere,[19] which is a development of the method of Kane.[20]

III. RESULTS

The rate integration algorithm has been applied to the bulk unstrained semiconductors GaAs, $In_{0.53}Ga_{0.47}As$ and $Si_{0.5}Ge_{0.5}$ (henceforth referred to as InGaAs and SiGe), all at 300 K. GaAs is an important semiconductor in the fabrication of high-speed devices, and InGaAs and SiGe have applications in the design of devices for optical communications. Although InGaAs and SiGe have rather narrower gaps than GaAs, they are all ''wide band gap'' in the sense that ionization thresholds lie at energies above the applicability of simple analytic band approximations. The band structure calculation for each material is performed using the nonlocal pseudopotential method of Chelikowski and Cohen.[17] Form factors and nonlocal well parameters for each material are given in Table I.

Rates and distributions of generated carriers are calculated and analyzed to determine factors affecting the behavior of the different materials. The influence of three factors on the behavior of the impact ionization rates in each material, particularly on the threshold softness, were examined: the role of variation in the matrix elements, the significance of the Γ valley in providing final states in the direct gap materials, and the effect of threshold anisotropy. Each of these is discussed below.

TABLE II. Fitted P-parameters for rates (P_r) and phase space (P_{ps}). Fit formula is: $R(E) = A(E - E_0)^P$ (with R in units of s^{-1} and E in eV).

	Material					
	GaAs		InGaAs		SiGe	
	P_r	P_{ps}	P_r	P_{ps}	P_r	P_{ps}
e^-	5.2	6.1	5.6	9.4	4.9	4.8
h^+	5.1	6.1	4.2	6.4	4.7	4.4

A. Role of matrix elements

The magnitude of the impact ionization rate can be considered to be determined by two factors: the area of the energy conserving surface in $\mathbf{k}_{1'}, \mathbf{k}_{2'}$ space, i.e., the volume of available phase space, and the average squared magnitude of the matrix elements throughout this phase space. This section examines the relative importance of each of these contributions. Impact ionization rates calculated using the algorithm described in Ref. 19 were approximated by a fit formula of the form

$$R(E) = A(E - E_0)^P, \quad (8)$$

where the parameters A, P and E_0 were adjusted to give the best straight line fit through $\log R$ vs $\log E$. The P parameter obtained is of interest as a higher value of P corresponds to a softer threshold.[21,22] Expressions of the form of Eq. (8) were also fitted to the volume of phase space (i.e., the rate calculated by setting the matrix elements to 1) for each material. Table II lists the P values obtained from the fits. In the case of the direct gap materials GaAs and InGaAs, the rate shows harder threshold behavior (i.e., a lower P value) than the corresponding volume of phase space for both electrons and holes. Conversely, electron and hole initiated rates in the indirect gap SiGe show quite similar (in fact, slightly softer) behavior than the corresponding phase space. Where the volume of phase space increases as a higher power of energy above threshold than the rate (i.e., as in the direct gap materials), it follows that the mean matrix element must be a decreasing function of the energy of the impacting carrier. Similarly, in SiGe the mean matrix element must be almost independent of the impacting carrier energy, increasing very slightly with respect to it. The cause of the matrix elements' dependence on the impacting carrier energy can be understood in terms of the variation in the mean momentum transfer occurring during collisions as a function of the energy of the initiating particle. Figure 1 plots the mean $\mathbf{q}$ transfer for transitions initiated by electrons in the first conduction band of each material. In the case of GaAs and InGaAs, the mean $\mathbf{q}$ transfer is an increasing function of the initiating electron's energy, while in SiGe it is more-or-less independent of this energy. The matrix element for a given transition depends on $\mathbf{q}$ roughly as

$$|M_{if}|^2 \propto 1/q^4. \quad (9)$$

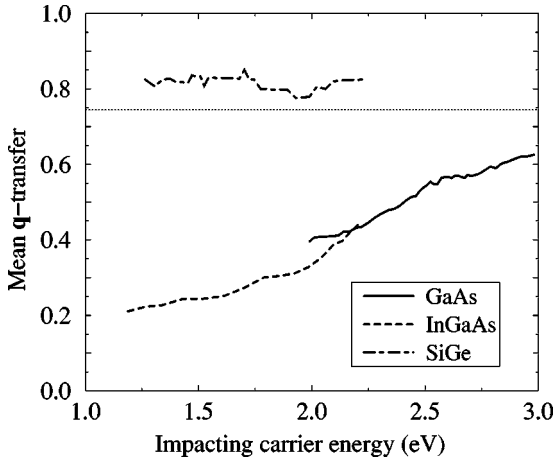

FIG. 1. Mean **q** transfer for transitions initiated by electrons in the first conduction band of each material. The horizontal line at $q \simeq 0.75$ indicates the mean value of q obtained by chosing transitions randomly in the first Brillouin zone.

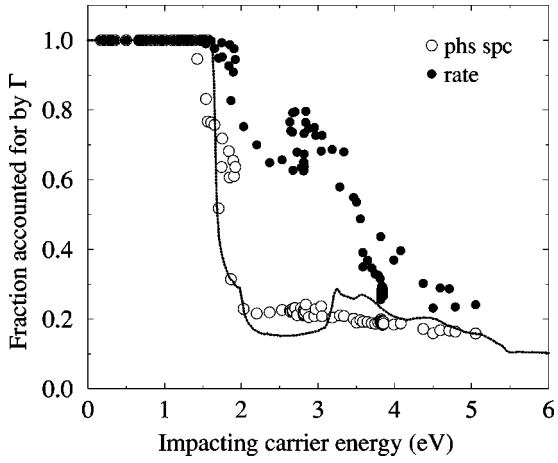

FIG. 3. Contribution of transitions involving the Γ valley as a fraction of all transitions to the rate and volume of phase space in InGaAs.

Thus, as the mean **q** transfer increases with increasing impacting carrier energy in the direct gap materials, so the mean matrix element falls, and hence the rate shows a harder energy dependence than the corresponding volume of phase space. Similarly, in SiGe the roughly constant mean **q** transfer leads to roughly constant mean matrix elements and hence the P parameters fitted to rate and phase space are approximately equal. This has implications for the use of the constant matrix element (CME) approximation which has occasionally been used to calculate rates.[23] Figure 2 compares rates calculated using the full expression for the matrix element and using the CME approximation in InGaAs and SiGe.

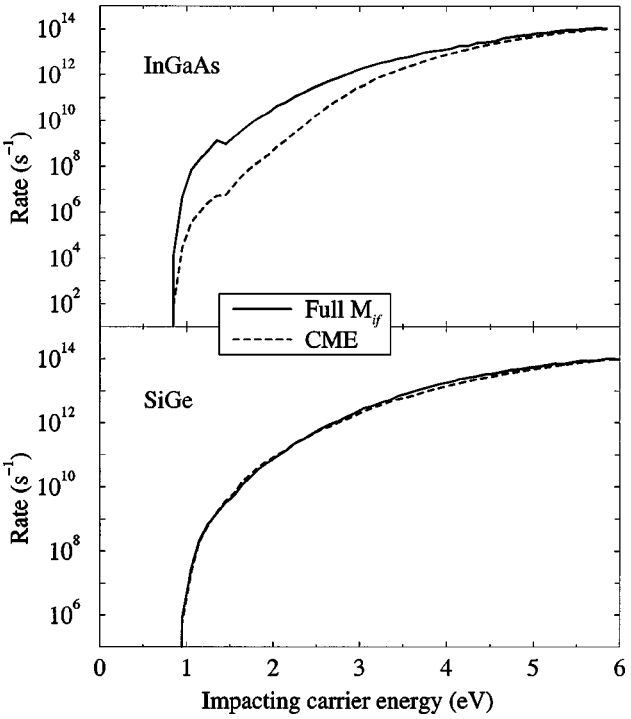

FIG. 2. Comparison of rates calculated for InGaAs and SiGe using the full expression for the matrix element and the CME approximation.

In each case the magnitude of the constant approximating the matrix elements has been chosen so as to give the same rate at high energy as that calculated using the full expression for M_{if}. In SiGe, the CME approximation is clearly excellent, giving rates close to those obtained using the full expression for the matrix element throughout the whole energy range plotted. In InGaAs however, the CME approximation badly underestimates the rate at low impacting carrier energy by up to 2 orders of magnitude, predicting softer threshold behavior. In GaAs, the CME approximation leads to a similar underestimation of the rate at low energy, though to less of an extent than in InGaAs. Although the analysis here has been applied to only three materials, it should generally be the case that in direct gap materials the use of the CME approximation will lead to overestimation of the threshold softness, particularly when the Γ valley lies well below the satellite valleys, and in indirect gap materials should provide more accurate results.

B. Influence of Γ valley on rate

The principle difference between the band structures of the indirect gap material SiGe and the direct gap materials GaAs and InGaAs is of course the existence in GaAs and InGaAs of a deep conduction band valley at Γ, which in SiGe is only very shallow. Having a light effective mass, the Γ valley does not provide a high density of states in comparison to the heavy effective mass satellite valleys, and it might therefore be expected that its influence on quantities involving integration over the Brillouin zone, such as the impact ionization rate, would be small. In fact the qualitative differences between the direct and indirect gap materials studied here, such as that described in Sec. III A, suggest that it is highly influential, and this is investigated here.

The solid circles plotted in Fig. 3 indicate what fraction of the total rate is accounted for by transitions in which one or both final states lie in the Γ valley. The open circles similarly represent the Γ valley's fractional contribution to the phase space. The dotted line is an estimate of the phase space provided by the Γ valley based on its three-dimensional den-

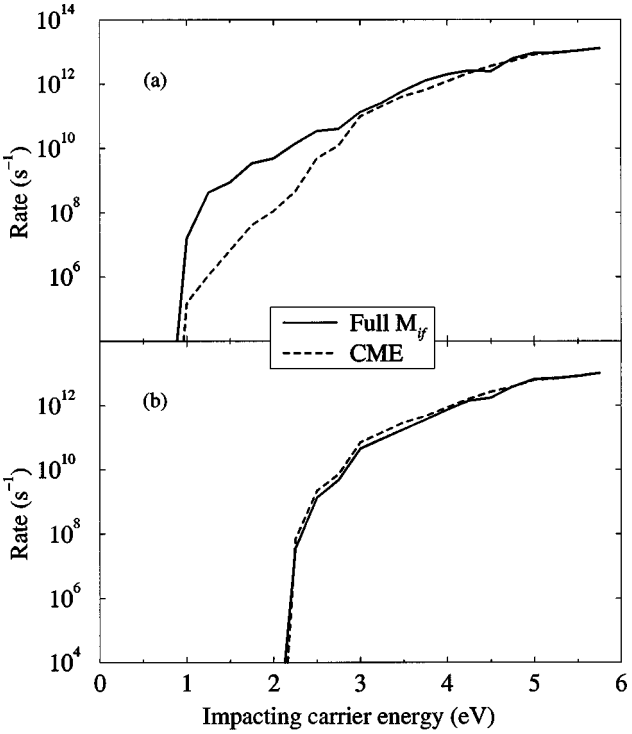

FIG. 4. Comparison of electron initiated rates in InGaAs, calculated using the full expression for the matrix element, and using the CME approximation. In (a), all transitions are included; in (b), those involving the Γ valley are excluded.

sity of states, and assuming the final state carrier energy E_f is related to the impacting carrier energy E_i by

$$E_f = \tfrac{1}{3}(E_i - E_{\text{gap}}), \tag{10}$$

which is based on the simplifying assumption that the three generated carriers share equally the energy made available by the impacting carrier. The plot shows that the fractional contribution of the Γ valley to the total volume of available phase space drops off rapidly once the heavier satellite valleys become accessible, and is approximately equal to the simple estimate for the value based on the three-dimensional density of states in this valley. However the fractional contribution to the rate remains much higher, accounting for the majority of transitions for impacting carriers up to about 3.5 eV. The fact that the Γ valley has a greater significance in influencing the total rate than would be expected from its contribution to the available phase space indicates that the corresponding matrix elements are higher. This is due to the low **q** transfer involved in transitions from the top of the valence band to states in the conduction band near Γ.

By excluding transitions to the Γ valley from the rate calculation, the behavior of the rate in each of the three materials studied here becomes very similar. Figure 4 compares electron initiated rates in InGaAs, calculated using the full expression for the matrix element, and using the CME approximation. In Fig. 4(a), the rate is calculated as normal, including contributions from all possible transitions. [Note, Figs. 2 and 4(a) are equivalent plots, but to reduce the required cpu time, Fig. 4 has been produced by including a reduced set of bands for the impacted and final states, hence the lower but qualitatively similar rates.] The rates in Fig. 4(b) have been calculated in a similar way, but excluding the contribution of transitions in which one or both final states lie in the Γ valley. In Fig. 4(a) the use of the CME approximation can be seen to lead to overestimation of the threshold softness, as discussed in Sec. III A. With final states provided by the Γ valley excluded, the accuracy of the CME approximation is seen to be considerably improved, as in SiGe. Table III compares fits of the expression, Eq. (8), obtained from the rates calculated using the full matrix element expression with and without final states in the Γ valley included. With transitions to the Γ valley included, the fitted expressions for the rates differ considerably. When final states in the Γ valley are excluded, the fitted expressions for each material, particularly the P values, become similar, indicating that the origin of differences in the behavior of the rates in each of these materials, in particular the threshold softness, is influenced almost entirely by the Γ valley, with the contribution of the rest of the band structure being similar for each material. This is in agreement with predictions of Bude and Hess[10] who have noted that thresholds are expected to be softer in materials in which the Γ satellite valley separation is larger and the band gap is smaller. Note that Allam[24] has pointed out that the materials studied here are all similar in that, although they have widely ranging band gaps, they each have a similar value of $\langle E_{\text{ind}} \rangle$, defined as

$$\langle E_{\text{ind}} \rangle = \tfrac{1}{8}(E_\Gamma + 3E_X + 4E_L), \tag{11}$$

where E_V is the energy gap between the top of the valence band and the bottom of the conduction band valley at V. Allam notes that InP, for example, has a larger value of $\langle E_{\text{ind}} \rangle$, and so should the analysis performed here of rates calculated with final states in the Γ valley excluded be applied to this material, similarities of the form seen in Table III might not be found.

TABLE III. Fitting parameters for electron initiated rates calculated by including all possible transitions, and by excluding transitions in which one or both final states lie in the Γ valley.

	Γ included			Γ excluded		
	A	P	E_0	A	P	E_0
GaAs	3.1×10^{09}	6.5	1.64	2.5×10^{10}	4.8	2.14
InGaAs	1.1×10^{08}	7.0	0.17	3.6×10^{10}	4.5	2.04
SiGe	1.4×10^{10}	4.4	0.87	1.4×10^{10}	4.4	0.87

C. Influence of anisotropy on threshold softness

Simple impact ionization models, such as that of Keldysh[25] which is based on algebraically defined band structure and has been used extensively in Monte Carlo transport simulations,[7,12] can be parametrized in terms of a single ionization threshold energy. A carrier in any state below the threshold energy is unable to initiate ionization, while a carrier in any state above it is. In real band structure

calculations, what is found instead is that the fraction of states from which ionization can be initiated increases from 0 to 1 over some finite energy range. The fraction $f(E_i)$ of ionizing states at E_i is given by

$$f(E_i)=\frac{\int t(\mathbf{k})\,\delta[E(\mathbf{k})-E_i]d^3\mathbf{k}}{\int \delta[E(\mathbf{k})-E_i]d^3\mathbf{k}}, \tag{12}$$

where $t(\mathbf{k})$ is defined as a function which is 1 if impact ionization can be initiated from state $\mathbf{k}$ and 0, otherwise. The range over which $0<f(E_i)<1$ is found to vary between materials and carrier types. A wider energy range corresponds to greater anisotropy, i.e., the threshold energy varies more with direction in $\mathbf{k}$ space.

The impact ionization rate is found to be an explicit function of the $\mathbf{k}$ vector of the ionizing carrier, with carriers at the same energy but different $\mathbf{k}$ vectors generally having widely varying rates. However, in a high field device carriers are likely to be spread throughout the Brillouin zone by phonon scattering,[7,13] with different $\mathbf{k}$ states at the same energy having approximately equal probabilities of being filled. Under these conditions, the rate of ionization which is normally an explicit function of the $\mathbf{k}$ vector, $R(\mathbf{k})$, can be characterized by a function of energy alone

$$R_{\mathrm{av}}(E_i)=\frac{\int R(\mathbf{k})\,\delta[E(\mathbf{k})-E_i]d^3\mathbf{k}}{\int \delta[E(\mathbf{k})-E_i]d^3\mathbf{k}}. \tag{13}$$

Thus $R_{\mathrm{av}}(E_i)$ is the average rate from all $\mathbf{k}$ states at energy E_i. However, a fraction $1-f(E_i)$ of these states cannot initiate impact ionization and hence these states lower the overall average ionization rate at energy E_i. If only the states which can initiate ionization are included in the ionization rate average, then a new rate R_{ion} is obtained such that

$$R_{\mathrm{av}}(E_i)=f(E_i)\times R_{\mathrm{ion}}(E_i). \tag{14}$$

Since $f(E_i)$ is a function which generally increases as E_i increases, it will have the effect of softening $R_{\mathrm{av}}(E_i)$ for a given $R_{\mathrm{ion}}(E_i)$.

Sano *et al.*[26] have investigated the behavior of $f(E_i)$ in Si and GaAs, finding that in Si the threshold is highly anisotropic, i.e., the energy range over which $f(E_i)$ rises from 0 to 1 is large, while in GaAs it is relatively isotropic. In Si the rate shows soft threshold behavior while in GaAs it is hard. This led Sano *et al.* to suggest that in each material $R_{\mathrm{ion}}(E_i)$ is in fact hard, and the different behavior of the actual ionization rate $R_{\mathrm{av}}(E_i)$ in each material is due mainly to variation in $f(E_i)$. They therefore propose a $\mathbf{k}$ vector dependent rate of the form

$$R(\mathbf{k})=U[E-E_0(\mathbf{k})] \tag{15}$$

for modeling impact ionization in Monte Carlo transport simulations,[8,9,11] where $U(x)$ is the unit step function $U(x)=0$ for $x<0$, $U(x)=1$ for $x\geqslant 0$ and $E_0(\mathbf{k})$ is a $\mathbf{k}$-dependent threshold energy.

A similar analysis performed here for SiGe and GaAs does not strongly support the use of such a model. Figure 5

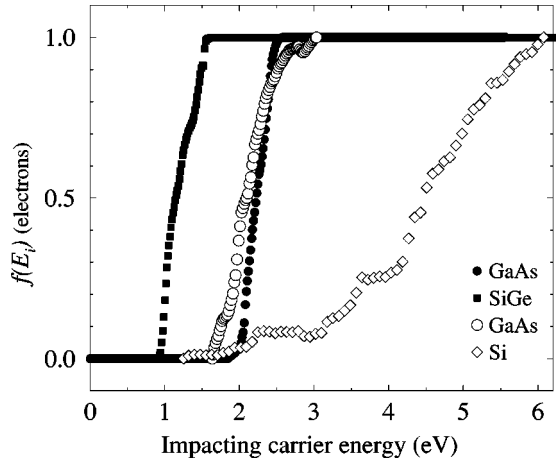

FIG. 5. Comparison of $f(E_i)$ calculated by Sano *et al.* (Ref. 26) for Si and GaAs (open symbols), and calculated here for SiGe and GaAs (filled symbols).

plots $f(E_i)$ calculated by Sano *et al.*[26] for Si and GaAs and calculated here for SiGe and GaAs. The plots for GaAs agree to within variations that are to be expected from differences in the band structure (Sano *et al.* employ the local pseudopotential method of Cohen and Bergstresser[27]). Since the lines plotted for Si and SiGe are for different materials, they are not strictly comparable. However, these two materials have similar band structures, both being indirect gap with the conduction band minimum near X, and each having either a very shallow or no Γ valley. The large difference between the behavior of $f(E_i)$ in each case is therefore surprising. Sano *et al.* have used the algorithm of Anderson and Crowell[28] to obtain the thresholds, which is known[10] to overestimate the threshold anisotropy. The algorithm used here is that of Beattie,[29] as applied to real band structure,[30] which has not been shown to suffer from such inaccuracies. It seems unlikely that Beattie's algorithm applied to Si would find the thresholds so anisotropic, and we conclude therefore that the results obtained here for the threshold anisotropy are to be preferred.

Figure 6 compares $R_{\mathrm{av}}(E_i)$ and $R_{\mathrm{ion}}(E_i)$ calculated for

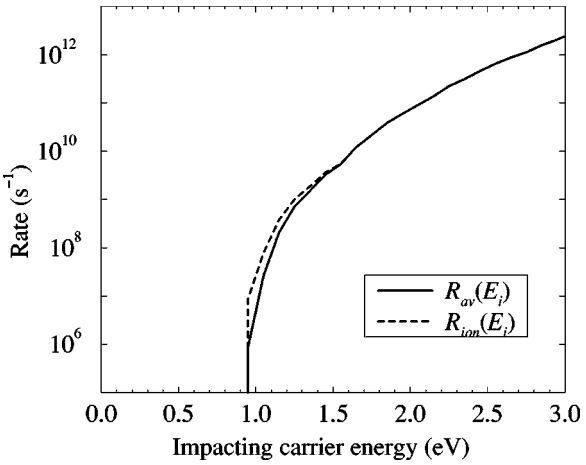

FIG. 6. Comparison of $R_{\mathrm{av}}(E_i)$ and $R_{\mathrm{ion}}(E_i)$ [calculated from Eqs. (13) and (14), respectively] for SiGe.

TABLE IV. Comparison of fits of Eq. (8) to $R_{av}(E_i)$ and $R_{ion}(E_i)$.

		Fit to $R_{av}(E_i)$			Fit to $R_{ion}(E_i)$	
		A	P	E_0	A	P
e^-	GaAs	1.4×10^{11}	5.2	1.89	2.0×10^{11}	4.7
	InGaAs	1.6×10^{10}	5.6	0.75	4.2×10^{10}	4.7
	SiGe	4.6×10^{10}	4.9	0.84	6.1×10^{10}	4.7
h^+	GaAs	8.2×10^{10}	5.1	1.43	9.0×10^{10}	5.0
	InGaAs	1.5×10^{11}	4.2	0.73	1.6×10^{11}	4.2
	SiGe	7.8×10^{10}	4.7	1.23	1.1×10^{11}	4.5

electrons in SiGe. The energy range in which R_{av} is lower than R_{ion} corresponds to the energy range in which $0<f(E_i)<1$. The effect of variation in $f(E_i)$ on the overall rate is not great. Table IV lists the parameters giving the best fit of Eq. (8) to R_{av} and R_{ion} for carriers in GaAs, InGaAs and SiGe. For the fit to R_{ion}, A and P were adjusted while the value of the threshold E_0 was fixed to be equal to that fitted to R_{av}. From the values presented in the table it can be seen that when only those states able to initiate ionization are included, mean rates for both types of carriers show harder threshold behavior, i.e., A increases and P decreases, as expected. However the changes in A and P are not particularly great (in comparison to the differences in these values between materials) confirming what can be seen in Fig. 6, i.e., that the effect of the anisotropy in the thresholds plays only a small role in softening the rates. In the case of the electron initiated rates it is interesting to note that the P parameter is the same for each material. This may be coincidental as there is no such correspondence in the behavior of the volume of phase space or mean matrix elements for these materials, and not too much significance should be read into this result. In any case, the softness of the threshold for R_{ion} still varies considerably between materials in that the fitted A parameters vary (with GaAs showing the hardest threshold behavior, i.e., the highest A value). Thus the effect of the anisotropy of the thresholds is not found here to greatly influence the softness of the threshold behavior of the rate in any of the materials, and the fact that the rates are soft, as opposed to the very hard behavior implied by the step function of Eq. (15), is due mainly to the dependence of the rate itself on impacting carrier energy, rather than the dependence of the fraction of carriers at that energy which are above threshold. It seems likely that Sano *et al.* have overestimated the anisotropy of the thresholds due to the use of Anderson and Crowell's threshold-finding algorithm.

IV. CONCLUSIONS

Impact ionization rates have been analyzed for the semiconductors GaAs, $In_{0.53}Ga_{0.47}As$ and $Si_{0.5}Ge_{0.5}$. In each material the effectiveness of the CME approximation in calculating the rate was tested. In SiGe, it was found to be a good approximation, reproducing the rates calculated using the full expression for the matrix element accurately at all energies. In GaAs and InGaAs the approximation was found to fail, particularly in InGaAs, predicting softer rates than were obtained using the full expression. The cause of the different behavior in the direct and indirect gap materials was found to be the mean momentum transfer occurring in transitions. In the indirect gap case, mean **q** transfer was found to be independent of impacting carrier energy, leading to mean matrix elements that were also independent. In the direct gap materials, mean **q** transfer was found to increase with increasing impacting carrier energy, leading to a corresponding decrease in mean of the matrix elements and hence the failure of the CME approximation.

The role of the Γ valley in influencing the behavior of the rate in the direct gap materials was examined and found to be greater than its small density of states would suggest. This was due to enhancement of matrix elements corresponding to transitions involving the Γ valley due to the low **q** transfer involved. With final states in the Γ valley excluded from the rate calculation, the behavior of the rate in the direct gap materials was found to become similar to that in SiGe, in that the CME approximation became accurate, and the degree of threshold softness was similar between the materials.

Finally, the role of anisotropy of the thresholds in determining the softness of the threshold behavior of the rate was investigated. While it was found that in all materials tested, threshold anisotropy acted to soften the thresholds, the effect was small, and the differing behavior of different materials is due to variation in the rate of increase of availability of final states as the impacting carrier energy increases above threshold. This is in contrast to the conclusions of Sano *et al.*[26] that thresholds in GaAs and Si are basically hard, but that the high degree of anisotropy in Si acts to soften the effective threshold.

ACKNOWLEDGMENTS

The authors would like to thank A. R. Beattie for several helpful discussions. One of the authors (D.H.) is grateful to the EPSRC(U.K.) for funding this work.

[1] S. M. Sze, *Semiconductor Devices, Physics and Technology* (Wiley, New York, 1985), Chap. 3.
[2] M. H. Somerville, J. A. del Alamo, and W. Hoke, IEEE Electron Device Lett. **17**, 473 (1996).
[3] H. Mizuno, M. Morifuji, K. Taniguchi and C. Hamaguchi, J. Appl. Phys. **74**, 1100 (1993).
[4] S. M. Sze, *Physics of Semiconductor Devices*, 2nd ed. (Wiley, New York, 1981).
[5] G. E. Stillman and C. M. Wolf, *Infrared Detectors II*, Semiconductors and Semimetals, Vol. 12 (Academic, New York, 1977), Chap. 5.
[6] F. Capasso, *Lightwave Communications Technology*, Semiconductors and Semimetals, Vol. 22 (Academic, New York, 1985), Chap. 1.
[7] H. Shichijo and K. Hess, Phys. Rev. B **23**, 4197 (1981).
[8] N. Sano, M. Tomizawa, and A. Yoshii, Appl. Phys. Lett. **56**, 653 (1990).
[9] N. Sano, T. Aoki, M. Tomizawa, and A. Yoshii, Phys. Rev. B **41**, 12122 (1990).
[10] J. Bude and K. Hess, J. Appl. Phys. **72**, 3554 (1992).
[11] V. Chandramouli and C. M. Maziar, Solid-State Electron. **36**, 285 (1993).
[12] J. Kolník, Y. Wang, I. H. Oğuzman, and K. F. Brennan, J. Appl. Phys. **76**, 3542 (1994).
[13] T. Kunikiyo, M. Takenaka, Y. Kamakura, M. Yamaji, H. Mizuno, M. Morifuji, and C. Hamaguchi, J. Appl. Phys. **75**, 297 (1994).
[14] I. H. Oğuzman, Y. Wang, J. Kolník, and K. F. Brennan, J. Appl. Phys. **77**, 225 (1995).
[15] P. T. Landsberg, *Recombination in Semiconductors* (Cambridge University Press, Cambridge, 1991).
[16] A. R. Beattie and P. T. Landsberg, Proc. R. Soc. London, Ser. A **249**, 16 (1959).

[17] J. R. Chelikowski and M. L. Cohen, Phys. Rev. B **14**, 556 (1976).
[18] J. P. Walter and M. L. Cohen, Phys. Rev. B **5**, 3101 (1972).
[19] D. Harrison, R. A. Abram, and S. Brand, J. Appl. Phys. **85**, 8178 (1999), preceding paper.
[20] E. O. Kane, Phys. Rev. **159**, 624 (1967).
[21] Y. Kamakura, H. Mizuno, M. Yamaji, M. Morifuji, K. Taniguchi, C. Hamaguchi, T. Kunikiyo, and M. Takenaka, J. Appl. Phys. **75**, 3500 (1994).
[22] T. Kunikiyo, M. Takenaka, M. Morifuji, K. Taniguchi, and C. Hamaguchi, J. Appl. Phys. **79**, 7718 (1996).
[23] N. Sano and A. Yoshii, J. Appl. Phys. **77**, 2020 (1995).
[24] J. Allam, Jpn. J. Appl. Phys., Part 1 **36**, 1529 (1997).
[25] L. V. Keldysh, Sov. Phys. JETP **10**, 509 (1960).
[26] N. Sano, T. Aoki, and A. Yoshii, Appl. Phys. Lett. **55**, 1418 (1989).
[27] M. L. Cohen and T. K. Bergstresser, Phys. Rev. **141**, 789 (1966).
[28] C. L. Anderson and C. R. Crowell, Phys. Rev. B **5**, 2267 (1972).
[29] A. R. Beattie, Semicond. Sci. Technol. **7**, 401 (1992).
[30] S. P. Wilson, S. Brand, A. R. Beattie, and R. A. Abram, Semicond. Sci. Technol. **8**, 1546 (1993).